IEEE Robotics and Automation Letters (RAL) paper presented at
2024 IEEE/RSJ International Conference on Intelligent Robots and Systems (IROS)
October 14-18, 2024. Abu Dhabi, UAE

The Design of a Layered Brain-Computer Interface System with Target Identification Module to Control Home Service Robot

Wenzhi Wang[1], Yuqing Mao[2] and Feng Duan[1]

***Abstract*—Brain-computer interface (BCI) systems, a kind of communication channel between human mind and the environment, turn brain activities into control commands. However, disabled people cannot withstand continuously high-tense operation of robots to fulfill complicated tasks. In order to simplify the operating process and strengthen the practicality of services, this paper proposed a layered BCI system integrated with a two-level target identification system to control a home service robot. We recorded single-channel steady-state visual evoked potentials (SSVEP) to diminish the number of electrodes in use. This hierarchical architecture can enhance the accuracy and sustainability during operation. The target identification system was established to reduce the burden of users and accelerate the service procedures. Subjects recruited in the experiment succeed in operating the robot to provide basic services. The average accuracy of online experiment is 87.38%. These results prove the effectiveness of this hierarchical system in operating a multifunctional home service robot with single-channel SSVEP, which plays an important role in both medical care and daily life.**

I. Introduction

Brain-computer interface (BCI) systems based on electroencephalogram (EEG) can obtain control commands from human mind, which enables the interaction between users and the external environment while relying on neither body language nor voice information [1]. BCI systems are typically utilized to command the service robots in an effort to address the daily challenges for the patients with mobility impairment caused by stroke or amyotrophic lateral sclerosis (ALS), spinal-cord injury, and other serious neuromuscular diseases or injuries [2]. The communication is regained and the life quality is improved thanks to BCI based on EGG [3].

BCI systems can be categorized into active, reactive and passive ones. The outputs of an active BCI system are derived from user's direct and conscious brain activity, and irrelevant from external events [4, 5]. Event-related desynchronization (ERD) and event-related synchronization (ERS) can be generated by motor imagery [6]. The EEG signals are subsequently extracted to classify the human intention and derive the control commands. However, the active BCI systems require users to be extensively trained in order to perform motor imagery tasks [7]. Meanwhile, the outputs of a passive BCI system are derived from arbitrary brain activity with no voluntary controlling purpose [8].

A reactive BCI system with external stimuli usually combines steady-state visual evoked potentials (SSVEP) with P300 [9]. The SSVEP, as a response to a repetitive visual stimulus at a fixed frequency, can be detected over the occipital cortex [10]. Different SSVEP signals can be generated and identified as the attention changes to the stimuli with different frequencies. The SSVEP-based BCI system can be used by most subjects because users need very little training to adapt to the systems [11]. Besides, unlike the internal signals, SSVEP signals are less susceptible to the electrical noise and the motion artifacts [12]. The SSVEP-based BCI systems are widely used since they perform better than the inertial way on both information transfer rate and signal-to-noise ratio [13]. SSVEP-based BCI systems are also more practical for people with eye movement disorder than eye trackers [14].

BCI systems with different architecture, like hierarchical ones and asynchronous ones, are proposed to improve the controllability and efficiency [15]. The hierarchical BCI systems proposed in [15] allows robot to independently accomplish low level tasks and use the assistant from users when facing high level tasks. Chae *et al*. applied an asynchronous direct-control system to implement the navigation of humanoid robot using an EEG based BCI [16].

In order to assist people in practical environment, the BCI-controlled robots are proposed [17]. Firstly, BCI can produce control commands for moving, which enables the paralyzes to manipulate their wheelchairs [18]. Secondly, BCI can manipulate the terminal effectors of robots to implement different functions like grasping and delivering [19]. The application of BCI controlled robots can bring great convenience to both medical care and daily life [20]. With the assistance of BCI controlled service robots, the disabled can implement daily tasks like fetching items without moving [21].

Despite the feasibility of controlling robots with pure BCI controlled systems, the sustainability can hardly be satisfied with the operating time increasing. To solve this problem

This research was supported by the National Natural Science Foundation of China (Key Program) (No. 11932013), and the Tianjin Science and Technology Plan Project (No. 22PTZWHZ00040). *(Corresponding author: Feng Duan).*

[1]W. Wang and F. Duan are with Tianjin Key Laboratory of Interventional Brain-Computer Interface and Intelligent Rehabilitation, Nankai University, Tianjin 300350, China (email: 2737441415@qq.com; duanf@nankai.edu.cn).

[2]Yuqing Mao is with the College of Letter and Science, University of California, Davis. 95618, United States (email: maotroy@outlook.com).

and improve the practicality, some other control strategies are employed, autonomous navigation for example [22]. To achieve most tasks in both medical care and daily life, the ability of detecting desired objects is very important. An object detection method with rapidity is proposed by Lee *et al* [23]. The algorithm is based on color histograms and local binary patterns (LBP), which correspondingly accomplish the rough target object detection and precise target object detection.

In our study, we control the robot with a layered asynchronous BCI system attached with a target identification module. Unlike some other researches which use many sensors to acquire EEG data, we reduced the number of sensors and improved efficiency through functional auxiliary modules. The layered architecture reduces number of stimuli while providing enough control commands.

The target identification module can recognize objects and detect the target. At the first level of the hierarchical architecture designed for the mobility task, users can navigate the robot to the destination. At the second level designed for the manipulation task, the users can give the order of grasping one target among three targets and delivering it to the desired place. Based on these, the system can be applied to manipulate a multifunctional service robot in both medical care and daily life.

II. Methods

A. System Overview

This layered SSVEP-based BCI system can command a service robot to perform common missions in its application scenarios as illustrated in Fig. 1. The visual stimulus and feedback can be presented by the LCD display.

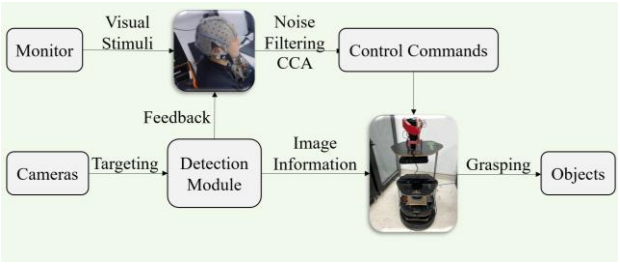

Fig. 1. The system overview. The SSVEP signals derived from the visual stimuli can be transferred into control commands, the robot fulfills the grasping task Correspondingly. The target detection module provides image information to the robot and visual feedback to the controller.

The SSVEP signals induced by the stimulus can be processed in order to achieve 10 kinds of commands. The subjects can use the commands to navigate the service robot and chose a target. The service robot then delivers the selected object into a dustbin autonomously.

B. Layered Architecture

The interface for presenting the hierarchical architecture is divided into two levels (see Fig. 2).

The first level contains five blocks and can be used to control the navigation of the service robot. When the robot arrives at the place suitable to grasp the objects, the user can use the "selection" to enter the next level.

The second level also contains five blocks and can be used to select one desired target among three options. When the selection is made, the user can confirm the decision for the robot to grasp the object. In case of mis-operation, the "return" function is provided to go back to the first level.

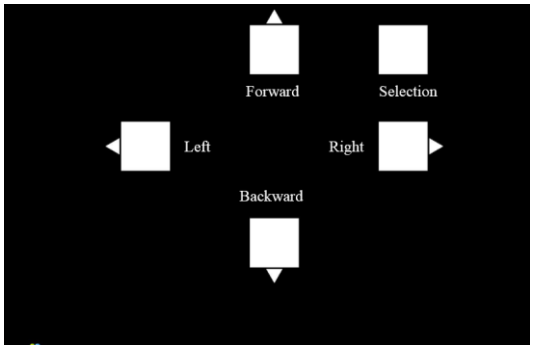

(a)

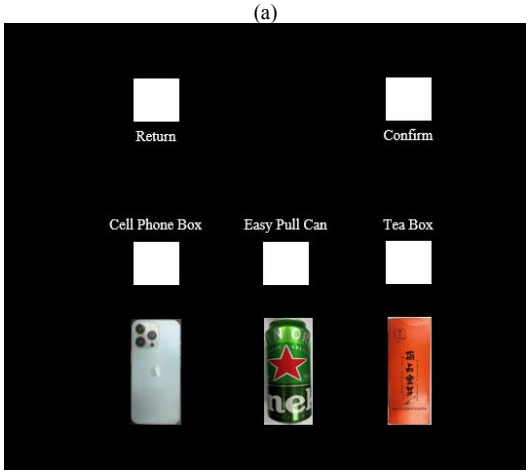

(b)

Fig. 2. Interface of the hierarchical architecture. (a) First level of the hierarchical interface: Robot navigation. (b) Second level of the hierarchical interface: Target selection.

TABLE I

Commands Generated According to Stimulus Frequency

Frequency (Hz)	First Level	Second Level
6	Forward	Return
7	Selection	Confirm
8	Left	Cell Phone Box
9	Right	Easy Pull Can
10	Backward	Tea Box

The word illustration does not appear on the screen during the experiment. The blocks are flickering at fixed and

distinctive frequencies. The relationship between the frequency and the function is listed as Table 1.

C. Stimulation

Frequency modulation carrier is usually used as SSVEP driving signals [24]. To generate stimuli signals at any frequency, we used the sampled sinusoidal method. In this work, the stimuli signal we used range from 6Hz to 10Hz.

The serial stimulus $s(f,i)$ can be generated by adjusting the monitor luminance, The relationship between the serial stimulus $s(f,i)$ and the refresh rate is indicated by the equation:

$$2s(f,i)-1=\sin[2\pi f(\frac{i}{x})], \tag{1}$$

where f means the frequency, i represents the frame index and x means the refresh rate. When the value of s is zero, the monitor is dark, while 1 corresponds to the lightest.

D. Data Processing

To record the EEG signal, we used an amplifier with 16 channels. We employed the international standard of 10-20 system (Fig.4) to set the electrodes. The impedances of electrodes were kept under 5 kΩ and the sampling rate was set to 256 Hz. A band-pass filter and a notch filter were employed in order to diminish the influence of external interfaces. As denoted in Fig. 3, the EEG signal is recorded by an active electrode at O_z. The ground electrode was set at F_{pz}, and the reference electrode was set at the right ear of the subjects.

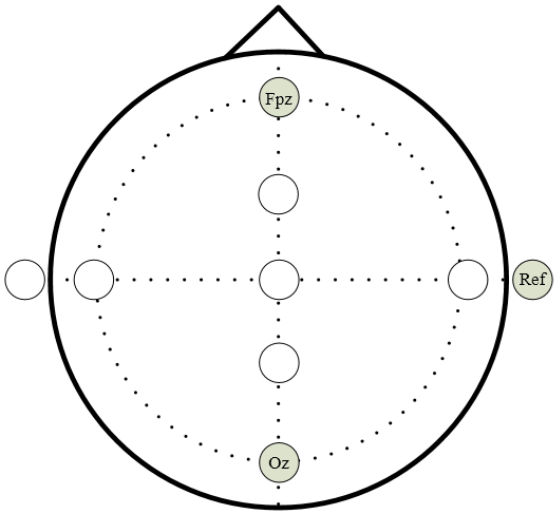

Fig. 3. EEG electrode position. The perspective is from the top of the head, where the triangle represents the nose.

After collecting the signal, we used the CCA (canonical correlation analysis) algorithm to generate the control commands from the flickering blocks in the two-level operation interface which contains five commands each.

CCA is a multivariate statistical method for measuring the correspondence between two distinct sets of variables. If there exist two stochastic variables, namely X and Y, CCA targets on finding two linear transformations w_x, w_y (the dimensions of which are equal to X, Y respectively) corresponding to two groups of variables, so as to maximize the correlation coefficient between two combined variables ($w_x^T X$, $w_y^T Y$) after linear transformation.

The CCA method was first used to detect SSVEP signals by Lin *et al* [25]. In our method, $X=[x_1,x_2,...,x_n]^T$ indicates the recorded signals from O_z. Y_i ,which has the same length with X, indicates the signals generated from the reference electrodes and can be calculated by:

$$Y_i=\begin{pmatrix}\sin(2\pi f_i t)\\ \cos(2\pi f_i t)\\ \cdots\\ \sin(2\pi k f_i t)\\ \cos(2\pi k f_i t)\end{pmatrix}, t=\frac{1}{F_s},\frac{2}{F_s},\ldots,\frac{N_s}{F_s} \tag{2}$$

where i indicates the number of targets, f_i indicates the frequency of the stimuli, N_s indicates the number of sample points and F_s means the sampling frequency.

The correlation coefficient between X and the reference signals under the stimuli f_i can be described as:

$$\rho(f_i)=\frac{E[x^T y_i]}{\sqrt{E[x^T x]E[y_i^T y_i]}}=\frac{E[\omega_x{}^T XY_i\omega_{Yi}]}{\sqrt{E[\omega_x{}^T XX^T\omega_x]E[\omega_{Yi}{}^T YY^T\omega_{Yi}]}} \tag{3}$$

The target stimulator's frequency can be identified by:

$$f_{target}=\max_{f_i}\rho(f_i),\ i=1,2,3...,M \tag{4}$$

where M indicates the amount of stimuli.

After identifying the signals, we delivered the propagated control commands to the robot.

E. Target Identification

To fulfill the function of grasping desired objects, we utilized a two-level detection system for target identification. As illustrated in Fig. 4, the detection system contains an upper system and a lower one.

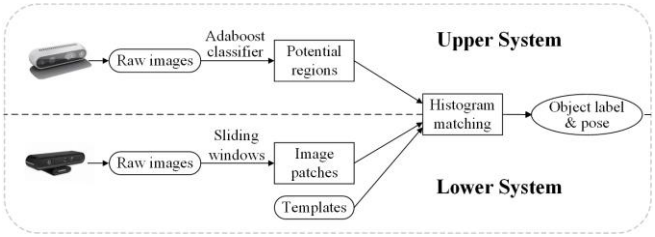

Fig. 4. Two-level detection system.

The upper system utilized an Orbbec RGB-D camera, which has a sensing range of 0.5-4.5m, to identify the targets for further grasping task. To extract the regions of targets, we used a classifier trained by the Adaboost algorithm. The training process focuses on the hue information and the input is the hue images of the entities, emanating from the hue component in the HSV chromaticity model. After extracting the regions, the KNN algorithm was utilized to analyze the distribution feature of the hue histogram. The histograms of the entities were portrayed in Figure 5.

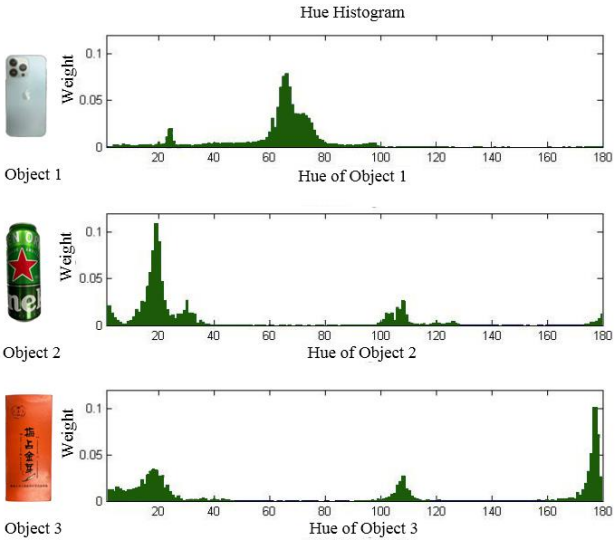

Fig. 5. The desired objects histograms.

In our system, considering the computational cost, we opted for a comprehensive examination of the resemblance between two histograms through the prism of the intersection of histograms. The histogram intersection distance is described by:

$$D(H_1, H_2) = \frac{\sum_{n=1}^{K} \min(H_1[n], H_2[n])}{\sum_{n=1}^{K} H_1[n]}, D \in (0,1) \qquad (5)$$

in which *H1* and *H2* means two different histograms and *K* means the amount of bins. To match the label of different objects, we set a threshold of $D(H_1, H_2)$. The object will be labeled if the maximum exceeds the threshold which was 0.4 in our experiment.

The lower system utilized an Intel RealSense D435i camera, which has a larger range of 0.11-10m. The lower system can fulfill the requirement of navigation due to its greater sensing range. We used a sliding window to segment the images. The template matching method was also utilized due to the easiness of detection single target. As for the matching, we used the same method as the upper system.

F. Robot Platform

Turtlebot is a widely used robot platform for its compatibility with ROS (Robot Operating System). In our research, we modified the Turtlebot by adding some functional modules to it, including an arm and two cameras.

The arm we used was a five-dof servo motor drove robot arm, which calculates the desired coordinates of each joint through inverse kinematics to accomplish the grasping tasks. The chassis was able to achieve all-round movements with a two-wheel drive system. The mobility of the chassis ensured the accomplishment of navigation. As for the cameras which provide visual information in both navigation and grasping, we have already introduced in the subsection above. Through the multi-functional module we utilized, our robot platform can meet the requirements of home service robots.

III. EXPERIMENTS

A. Experimental Participants

Five participants were selected for the study and assigned the names P1 to P5. P2 and P4 had prior knowledge of SSVEP, while P1, P3, and P5 were unfamiliar with the BCI system. The participants took part in two distinctive experiments, completed on separate occasions, one in the virtual realm and the other in the physical world, and they were fully briefed on the entire procedure before the commencement of the experiments. Additionally, all participants provided informed consent prior to taking part in the study. Participants were instructed to sit in a proper posture to look at the display.

B. Offline Performance

1) Procedure

The objective of this in-person trial was to assess the precision of pinpointing SSVEP targets. The test involved displaying visual cues comprising of seven flickering blocks to the participants. The start of the recording was indicated by the use of a crisp tone. Every participant completed a total of 15 recording sessions, where their gaze was fixed upon each of the 7 flickers for a duration of 15 seconds in each session. As a result, there were a total of 15 signal segments, each lasting 15 seconds, recorded for each focal point. The subjects were given a one-minute break between every session to alleviate eye fatigue.

2) Results

For each target, the CCA was executed utilizing 15 seconds of EEG data as a signal input overlaying a corresponding sinusoid waveform containing harmonics, as a reference input. The classification outcome has been tabulated in Table II, which is indicative of the performance exhibited by the CCA methodology in this BCI system.

TABLE II

SUCCESSFUL RECOGNITION RATE OF FIVE KINDS OF SSVEP SIGNALS METHOD

Subject	Frequency						
	6Hz(%)	7Hz(%)	8Hz(%)	9Hz(%)	10Hz(%)	Mean(%)	SD
P1	80.00	93.33	100.00	86.67	100.00	92.00	8.96
P2	80.00	93.33	93.33	86.67	100.00	90.67	7.60
P3	100.00	100.00	100.00	100.00	100.00	100.00	0
P4	100.00	73.33	100.00	80.00	100.00	90.67	13.00
P5	100.00	100.00	100.00	80.00	100.00	96.00	8.94

For the purposes of ascertaining the efficacy of the mechanisms enlisted, it was deemed expedient to gauge the classifying accuracy, thereby rendering it a metric for evaluation. Given the aggregated data of seven test subjects, the resultant average emerged over 90%.

Based on the empirical outcomes, it is apparent that the identification accuracy rates were highly favorable for 8 and 10 Hz frequencies. When the stimulation frequency is 10Hz, SSVEP produces the maximum response. These outcomes display promise and provide the foundation to proceed with online experimentation. Table III represents the confusion matrix, an effective technique to assess the discrimination result in pattern recognition studies, aimed at identifying any possible instances of mislabeling.

TABLE III

THE CCA CONFUSION MATRIX FOR CLASSIFICATION

Actual Frequency	Identified Frequency				
	6Hz	7Hz	8Hz	9Hz	10Hz
6Hz	92.00	1.33	1.33	2.67	2.67
7Hz	1.33	92.00	4.00	1.33	1.33
8Hz	-	1.33	98.67	-	-
9Hz	10.67	1.33	1.33	86.67	-
10Hz	-	-	-	-	100.00

C. Online Performance

1) Environment

As depicted in Figure 6, the entire test was conducted within an enclosed chamber. A ceiling-mounted camera was utilized to track the robot's trajectory, while participants were directed to position themselves in front of the desk. There, three different objects were arranged atop the table situated by the wall. Moreover, a trash bin was positioned at the corner of the room.

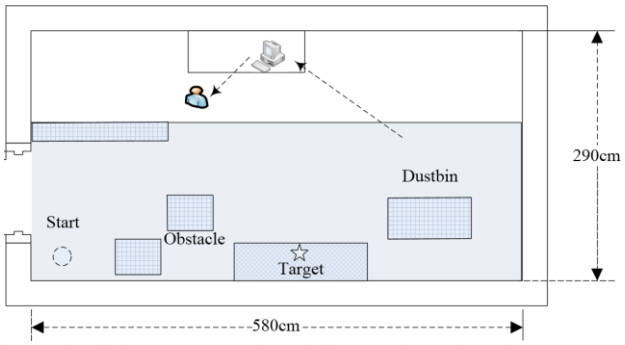

Fig. 6. The bird's eye perspective of the experimental environment. Each subject was required to fulfill the experiment four times. Varying degrees of luminosity were recorded and analyzed with the aid of a video camera disposed on a ceiling mount. The relative shade, which served as a corollary of this process, was projected onto an LCD display, serving as visual feedback for the test subjects.

2) Procedure

During this trial, the individuals were tasked with guiding the TurtleBot to its destination, while concurrently selecting a predetermined target. Each of the four iterations entailed a fresh starting point for the participants. To make calculated decisions, the participants relied on the visual input registered on the overhead camera. Upon confirmation of the target, TurtleBot then independently executed the delivery service. The entire process of manipulating the robot is depicted in Fig. 7.

Commands were generated at a frequency of every 5s. Within the first 4s, subjects were required to select one flicker to gaze at, while in the remaining 1 second, ascertaining which flicker to concentrate on next,

so as to realize the desired outcome, required a cursory examination of the camera monitor. The CCA target identification method utilized the 4s EEG data to generate the corresponding command.

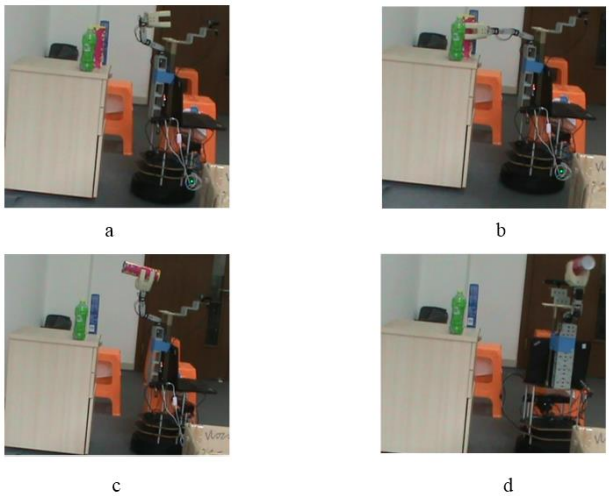

Fig. 7. The process of manipulation services. After the identification process in (a), the Turtlebot robot grasps the objects selected by controller in (b)(c) and then deliver it to destination in (d).

3) Results

TABLE IV

CLASSIFICATION ACCURACY OF SSVEP OF ONLINE EXPERIMENT

Subject	Trial 1(%)	Trial 2(%)	Trial 3(%)	Trial 4(%)	Mean(%)	SD
P1	100.00	84.00	79.48	78.72	85.55	9.90
P2	82.75	83.87	73.68	82.14	80.61	4.68
P3	82.14	85.71	94.74	90.91	88.38	5.56
P4	88.89	80.00	84.62	80.65	83.54	4.11
P5	95.23	100.00	100.00	100.00	98.81	2.38

TABLE V

TIME COST OF ONLINE EXPERIMENT

Subject	Trial 1(%)	Trial 2(%)	Trial 3(%)	Trial 4(%)	Mean(%)	SD
P1	85.00	125.00	195.00	135.00	160.00	67.58
P2	145.00	155.00	285.00	140.00	181.25	69.45
P3	140.00	140.00	95.00	110.00	121.25	22.50
P4	135.00	150.00	130.00	155.00	142.50	11.90
P5	105.00	115.00	100.00	105.00	106.25	2.38

Subjects were tasked with exercising their decision-making process by focusing their attention on the associated stimulus. The BCI system would then send the command to the robot. Correct commands were counted only if they were in alignment with the decision made by the subjects.

The results of the SSVEP's online classification accuracy are displayed in Table IV, where it is evident that the average identification accuracy was found to be 87.38%. Subjects P2 and P4, who had prior experience with the BCI system, achieved an average accuracy rate of 80.61% and 83.54%, respectively. Despite being new to the BCI system, subject P5 achieved an impressive accuracy rate of 98.81%.

Table V presents the time cost associated with online experimentation. This cost is based on the number of commands issued, with each command being generated at an interval of 5 seconds as per the experimental design. The average time cost observed over five subjects was found to be 142 seconds.

In order to evaluate the effectiveness of the SSVEP-based BCI system under study, we compared our results with those obtained from previous studies on BCI-controlled robots as presented in Table VI. Our system has the best efficiency by fulfilling ten commands with only one electrode.

Our BCI system recorded SSVEP signals using a single electrode. The participants were able to successfully issue ten control-oriented commands to operate a service robot offering three fundamental services.

IV. CONCLUSION

The present paper details the development of a system utilizing SSVEP signals in conjunction with a BCI to control the robot. In contradistinction to antecedent investigations predicated upon the utilization of a convoluted EEG-based mechanism as a means of furnishing an adequate profusion of commands, we have employed an individual electrode aimed at capturing SSVEP signals, and in consequence have created ten distinct commands for the purposes of directing the robot's operation. Our intention in proffering such a system was to bestow upon users the power to employ the robot for purposes of mobility, manipulation, and delivery, whereby users may guide the robot in four cardinal directions, designate an object for the robot to take hold of, and avail themselves of visual servo controls that amplify versatility whilst shortening task time. This particular BCI system predicated upon SSVEPs offers a highly efficacious alternative to other alternatives on the market, as it requires but few channels while simultaneously encompassing a broader ambit of activities.

Our system provides an efficient way of controlling a home service robot, the disabled can control the robot with only their eyes, the robot can then move to the destination, grasp the desired object and then deliver it to the user. In home service scenarios, the object can be most of the daily used items like cups, books and remote controllers.

Although we use only one electrode to improve the efficiency in this study, we can still improve our accuracy by adding more electrodes. Meanwhile, although we have succored the effectiveness of this BCI system through inquiry conducted upon healthy beings, further experimentation carried out upon individuals afflicted with motility-related diseases will be required in order to ascertain the system's comprehensive universality.

TABLE VI

COMPARISON BETWEEN PREVIOUS METHODS AND OURS ABOUT BCI-BASED ROBOTS

Author	NUM. OF ELECTRODES	NUM. OF COMMANDS	FUNCTION	EEG	ACCURACY OF SSVEP	REFERENCE
Zhang	15	8	moving	SSVEP	90.37%	[18]
Muller	12	4	moving	SSVEP	92.00%	[26]
Diez	3	4	moving	SSVEP	95.00%	[27]
This work	1	10	moving, grasping, delivering.	SSVEP	87.38%	This work

REFERENCES

[1] S. Chaudhary, S. Taran, V. Bajaj, and S. Siuly, "A flexible analytic wavelet transform based approach for motor-imagery tasks classification in BCI applications," *Comput. Methods Programs Biomed.*, vol. 187, pp. 105325, 2020.

[2] F. Wang, Y. Wen, J. Bi, H. Li, J. Sun, "A portable SSVEP-BCI system for rehabilitation exoskeleton in augmented reality environment", *Biomed. Signal Process. Control*, vol. 83, pp. 104664, 2023.

[3] Rui Na, Chun Hu, Ying Sun, Shuai Wang, Shuailei Zhang, Mingzhe Han, Wenhan Yin, Jun Zhang, Xinlei Chen, Dezhi Zheng, "Reprint of: An embedded lightweight SSVEP-BCI electric wheelchair with hybrid stimulator,". *Digit. Signal Process.* vol. 125, pp. 103573, 2022.

[4] F. Dehais, S. Ladouce, L. Darmet, TV. Nong, G. Ferraro, J. Torre Tresols, S. Velut, P. Labedan, "Dual passive reactive brain-computer interface: A novel approach to human-machine symbiosis," *Front. Neuroergon.*, vol. 3, pp. 824780, 2020.

[5] T. O. Zander and L. R. Krol, "Team PhyPA: Brain-Computer Interfacing for Everyday Human-Computer Interaction," *Period. Polytech. Electr. Eng. Comput*, vol. 61, no. 2, pp. 209-216, 2017.

[6] L. F. Velásquez-Martínez, J. Caicedo-Acosta, G. Castellanos-Domínguez, "Entropy-Based Estimation of Event-Related De/Synchronization in Motor Imagery Using Vector-Quantized Patterns," *Entropy*, vol. 22, no. 6, pp. 703, 2020.

[7] N. Padfield, J. Zabalza, H. Zhao, V. M. Vargas, J. Ren, "EEG-Based Brain-Computer Interfaces Using Motor-Imagery: Techniques and Challenges," *Sensors*, vol. 19, no. 6, pp. 1423, 2019.

[8] F. M. Toma, "A hybrid neuro-experimental decision support system to classify overconfidence and performance in a simulated bubble using a passive BCI," *Expert Syst*, vol. 212, pp. 118722, 2023.

[9] D. Wen, B. Liang, Y. Zhou, H. Chen, T. Jung, "The Current Research of Combining Multi-Modal Brain-Computer Interfaces With Virtual Reality ," *IEEE J. Biomed. Health Informatics*, VOL. 25, NO. 9, PP. 3278-3287, 2021.

[10] T. Tsoneva, G. Garcia-Molina, P. Desain , "SSVEP phase synchronies and propagation during repetitive visual stimulation at high frequencies," *Sci Rep*, vol. 11, pp. 4975, 2021.

[11] X. Chen, B. Liu, Y. Wang, H. Cui, J. Dong, R. Ma, N. Li, X. Gao, "Optimizing stimulus frequency ranges for building a high-rate high frequency SSVEP-BCI," *IEEE Trans. Neural Syst. Rehabilitation Eng.*, vol. 31, pp. 1277-1286, 2023.

[12] A. Liu, Q. Liu, X. Zhang, X. Chen, X. Chen, "Muscle artifact removal toward mobile SSVEP-based BCI: A comparative study," *IEEE Trans. Instrum.*, vol. 70, pp. 1-12, 2021.

[13] R. Chen, G. Xu, J. Pei, Y. Gao, S. Zhang, C. Han, "Typical stochastic resonance models and their applications in steady-state visual evoked potential detection technology ," *Expert Syst. Appl*, vol. 225, pp. 120141, 2023.

[14] A. Saboor, M. Benda, A. Rezeika, R. Grichnik, F. Gembler, P. Stawicki, I. Volosyak., "Mesh of SSVEP-Based BCI and Eye-Tracker for Use of Higher Frequency Stimuli and Lower Number of EEG Channels," in *FIT 2018*, pp. 99–104, 2018.

[15] I. Akinola, B. Chen, J. Koss, A. Patankar, J. Varley, and P. Allen, "Task level hierarchical system for BCI-enabled shared autonomy," in *Humanoids 2017*, pp. 219–225, 2017.

[16] Y. Chae, J. Jeong, and S. Jo, "Toward Brain-Actuated Humanoid Robots: Asynchronous Direct Control Using an EEG-Based BCI," *IEEE Trans. Robotics*, vol. 28, no. 5, pp. 1131-1144, 2012.

[17] L. Chen, P. Chen, S. Zhao, Z. Luo, W. Chen, Y. Pei, H. Zhao, J. Jiang, M. Xu, Y. Yan, E. Yin, "Adaptive asynchronous control system of robotic arm based on augmented reality-assisted brain–computer interface," *J. Neural Eng.*, vol. 18, no. 6, pp. 066005, 2021.

[18] Z. Zhang, W. Wang, P. Song, S. Sheng, L. Xie, F. Duan, Y. Guansoo, M. Odagaki, "Design of an SSVEP-based BCI System with Vision Assisted Navigation Module for the Cooperative Control of Multiple Robots," in *CYBER 2017*, pp. 558–563, 2017.

[19] J. Mang, Z. Xu, Y. Qi, T. Zhang, "Favoring the cognitive-motor process in the closed-loop of BCI mediated post stroke motor function recovery: challenges and approaches," *Frontiers Neurorobotics*, vol. 17, 2023.

[20] A. N. Belkacem, N. Jamil, J. A. Palmer, S. Ouhbi, C. Chen, "Brain computer interfaces for improving the quality of life of older adults and elderly patients," *Front. Neurosci.*, vol. 14, 2020.

[21] R. Zhang, S. Lee, M. Hwang, A. Hiranaka, C. Wang, W. Ai, J. J. R. Tan, S. Gupta, Y. Hao, G. Levine, R. Gao, A. Norcia,F. F. Li, J. Wu, "Noir: Neural signal operated intelligent robots for everyday activities," in *CoRL 2023*, pp. 1737-1760, 2023.

[22] M. Li, R. Wei, Z. Zhang, P. Zhang, G. Xu, W. Liao, "CVT-based asynchronous BCI for brain-controlled robot navigation," *Cyborg Bionic Syst.*, vol. 4, 2023

[23] K. Lee, C. Lee, S. A. Kim, and Y. H. Kim, "Fast object detection based on color histograms and local binary patterns," in *TENCON 2012 IEEE Region 10 Conf.*, pp. 1–4, 2012.

[24] D. Zhao, X. Li, X. Hou, M. Feng, R. Jiang, "Synchrosqueezing with short-time fourier transform method for trinary frequency shift keying encoded SSVEP," *Technol. Health Care*, vol. 29, no. 3, pp. 505-519, 2021.

[25] Z. Lin, C. Zhang, W. Wu, and X. Gao, "Frequency Recognition Based on Canonical Correlation Analysis for SSVEP-Based BCIs," *IEEE Transactions on Biomedical Engineering*, vol. 53, no. 12, pp. 2610–2614, 2006.

[26] S. M. T. Muller, W. C. Celeste, T. F. Bastos-Filho, M. Sarcinelli-Filho, "Brian-Computer interface based on visual evoked potentials to command autonomous robotic wheelchair," *Journal of Medical and Biological Engineering*, vol. 30, no. 6, pp. 407-416, 2010.

[27] P. F. Diez, S. M. T. Müller, V. A. Mut, E. Laciar, E. Avila, T. F. B. Filho, M. S. Filho, "Commanding a robotic wheelchair with a high-frequency steady-state visual evoked potential based brain–computer interface," *Med. Eng. Phys.*, vol. 35, no. 8, pp. 1155–1164, 2013.